Author Manuscript

Author Manuscript

Author Manuscript

Author Manuscript

HHS Public Access

Author manuscript

*Brain Struct Funct*. Author manuscript; available in PMC 2018 December 03.

Published in final edited form as:

*Brain Struct Funct*. 2017 March ; 222(2): 1039–1052. doi:10.1007/s00429-016-1263-4.

# Sensory and motor cortex function contributes to symptom severity in spinocerebellar ataxia type 6

**Nyeonju Kang**[1], **Evangelos A. Christou**[1], **Roxana G. Burciu**[1], **Jae Woo Chung**[1], **Jesse C. DeSimone**[1], **Edward Ofori**[1], **Tetsuo Ashizawa**[2], **Sankarasubramon H. Subramony**[2], and **David E. Vaillancourt**[1,2,3]

[1]Department of Applied Physiology and Kinesiology, University of Florida, P.O. Box 118205, Gainesville, FL 32611-8205, USA

[2]Department of Neurology, University of Florida, Gainesville, USA

[3]Department of Biomedical Engineering, University of Florida, Gainesville, USA

## Abstract

Spinocerebellar ataxia type 6 (SCA6) is a genetic disease that causes degeneration of Purkinje cells, and recent evidence points to degeneration of Betz cells in the motor cortex. The relation between functional activity of motor cortex and symptom severity during a hand-grip motor control in vivo has not yet been investigated. This study explored both functional changes in the sensorimotor cortex and cerebellar regions and structural alterations in the cerebellum for SCA6 patients as compared to age-matched healthy controls using a multimodal imaging approach (task-based fMRI, task-based functional connectivity, and free-water diffusion MRI). Further, we tested their relation with the severity of ataxia symptoms. SCA6 patients had reduced functional activity in the sensorimotor cortex, supplementary motor area (SMA), cerebellar vermis, and cerebellar lobules I-VI (corrected $P < 0.05$). Reduced task-based functional connectivity between cortical motor regions (i.e., primary motor cortex and SMA) and cerebellar regions (i.e., vermis and lobules I–VI) was found in SCA6 (corrected $P < 0.05$). SCA6 had elevated free-water values throughout the cerebellum as compared with controls (corrected $P < 0.05$). Importantly, reduced functional activity in the sensorimotor cortex and SMA and increased free-water in the superior cerebellar peduncle and cerebellar lobule V were related to more severe symptoms in SCA6 (all pairs: $R^2 \geq 0.4$ and corrected $P < 0.05$). Current results demonstrate that impaired functional activity in sensorimotor cortex and SMA and elevated free-water of lobule V and superior cerebellar peduncle are both related to symptom severity, and may provide candidate biomarkers for SCA6.

### Keywords

Diffusion MRI; Functional MRI; Spinocerebellar ataxia type 6; Free-water; Task-based functional connectivity

Compliance with ethical standards

**Conflict of interest** The authors declare that they have no conflict of interest.

**Electronic supplementary material** The online version of this article (doi:10.1007/s00429-016-1263-4) contains supplementary material, which is available to authorized users.

Author Manuscript Author Manuscript Author Manuscript Author Manuscript

## Introduction

Spinocerebellar ataxia type 6 (SCA6) is a late onset auto-somal dominant disorder caused by a CAG expansion mutation in the a subunit of the neuronal calcium channel gene, leading to degeneration of Purkinje cells and progressive motor and behavioral impairments (Ilg et al. 2007; Solodkin and Gomez 2012). Common motor disabilities in SCA6 involve deficits in movement coordination of upper and lower extremities, and impaired walking and balance (Bastian 2006; Morton and Bastian 2004; Shadmehr and Krakauer 2008). Previous structural magnetic resonance imaging and pathology studies have found degeneration in the cerebellum in SCA6 (Reetz et al. 2013; Seidel et al. 2012; Tuite and Dagher 2013). Although some evidence suggest cerebello-cortical interactions (Bernard et al. 2012, 2014; Gierga et al. 2009; Middleton and Strick 2000; Watson et al. 2014), little is known about how degenerationof the cerebellum influences pathways to the motor cortex in vivo.

There is evidence that SCA6 patients with mild and severe symptoms exhibit greater activity in the lateral cerebellum, whereas presymptomatic patients exhibit greater activity in the vermis (Falcon et al. 2015). A single tensor diffusion analysis model revealed reduced fractional anisotropy (FA) values in the cerebral peduncle and middle cerebellar peduncle, and only the decreased FA in the middle cerebellar peduncle was correlated with more severe disease symptoms. In addition, the authors reported a network-level change in SCA6 such that effective connectivity between visual-related cortical regions (i.e., frontal eye fields, inferior and superior parietal lobules, visual association areas, and visual-temporal occipital areas) and intermediate and lateral cerebellum was reduced in individuals with severe disease symptoms in comparison to healthy controls and presymptomatic and mild patients. While these initial findings suggest that oculomotor and visual regions have impaired connectivity in SCA6, we still know very little about motor control in SCA6 and how functional activity in the motor cortex, sensory cortex, and cerebellum relate to symptom severity in SCA6.

The current study examines upper limb motor function using a hand-grip force control task in SCA6 and control individuals. Using a grip force control fMRI paradigm (Neely et al. 2015; Planetta et al. 2015a; Spraker et al. 2010), we explored task-based fMRI activity within sensory and motor cortex and cerebellum, and task-based functional connectivity between cortical motor regions (i.e., sensorimotor cortex and supplementary motor area: SMA) and cerebellum. In addition, free-water diffusion magnetic resonance imaging (dMRI) was assessed using a bi-tensor model to evaluate the tissue compartment and the free-water compartment within cerebellar regions (i.e., dentate, cerebellar lobules V and VI, cerebellar vermis, and peduncles). Moreover, we examined the relation of functional activity in the sensorimotor cortex, SMA, and cerebellum and structural changes in the cerebellum to symptom severity in SCA6.

Author Manuscript Author Manuscript Author Manuscript Author Manuscript

## Materials and methods

### Participants

Twenty-eight individuals participated in this study: 14 patients who were diagnosed and genetically confirmed with SCA6 (mean age = 63.6 years and SD = 6.8 years; 10 females and 4 males) and 14 age-matched healthy controls (mean age = 65.8 years and SD = 7.9 years; 10 females and 4 males). Age at diagnosis ranged from 35 to 75 years (mean age = 59.4 years and SD = 10.2 years). Mean time since diagnosis was 6.6 years (SD = 6.9 years). Clinical severity of ataxic symptoms for SCA6 patients was estimated using International Cooperative Ataxia Rating Scale (ICARS) and Scale for the Assessment and Rating of Ataxia (SARA), and blinded to the imaging data. Table 1 displays demographics of all participants. Healthy control individuals had no neurological impairments and cognitive deficits (Montreal Cognitive Assessment: MoCA: mean = 27.4 and SD = 1.5). Handedness for all participants was self-reported. Prior to testing, all participants read and signed an informed consent form approved by Institutional Review Board of the University of Florida.

### Pinch grip force task

We selected a well-established pinch grip force control paradigm (Fig. 1a) because previous studies have shown reliable blood oxygen level-dependent (BOLD) activity changes in individuals with neurological disorders that include Parkinson’s disease, essential tremor, multiple system atrophy, and progressive supranuclear palsy (Burciu et al. 2015; Neely et al. 2015; Planetta et al. 2015a; Spraker et al. 2010). Further, our pilot data confirmed that SCA6 patients were able to execute pinch grip force with similar behavioral performance as age-matched healthy controls.

Before entering the MRI scanner, we tested maximum voluntary contraction (MVC) for pinch grip force. SCA6 used their more affected hand, which was self-reported, and controls produced force with either the dominant or non-dominant hand, assigned randomly. All participants practiced for 30 min outside the MRI scanner, to become familiar with the task. During MRI acquisition, a pinch grip force task was administered using a custom LabVIEW program (National Instruments, Austin, TX, USA). A custom-designed MRI-compatible fiber optic transducer with a resolution of 0.025 N (Neuroimaging Solutions, Gainesville, FL, USA; Fig. 1a) was used for collecting pinch grip force data. Participants completed one 7 min 20 s pinch grip force task (Fig. 1b). During the block-design session, visual feedback was shown on the LCD monitor via a mirror mounted on the head coil. As shown in Fig. 1, the scan included a force with visual feedback block, force without visual feedback block, and rest. During force block the subject produced 10 force pulses lasting 2 s each, with 1 s of relaxation (Fig. 1c). For each force pulse the subject was required to produce force at 15 % of the MVC. The force pulse was cued by the red bar turning to green (Fig. 1d), and the pinch and hold periods lasted 2 s followed by the green bar turning back to red, which cued the subject to relax force. During the force blocks, subjects experienced the vision block and no vision block. In the vision block, the green bar moved vertically providing online feedback of the amount of force produced. In the no vision block, the green bar did not move, and the subject had to produce the force from memory. We did not have a specific hypothesis for the vision and no vision blocks, and we used this paradigm because it is well-

Author Manuscript Author Manuscript Author Manuscript Author Manuscript

validated in prior studies and the paradigm elicits a robust BOLD signal across the cortex, basal ganglia, thalamus, and cerebellum (Burciu et al. 2015; Neely et al. 2015; Planetta et al. 2015a). Participants completed eight total blocks (four vision and four no-vision) during the fMRI session.

### fMRI acquisition

We collected fMRI using a 3-T Philips Medical Systems MRI scanner (Achieva; 32-channel head coil) that met routine quality assurance at the McKnight Brain Institute. Based on a $T_2$*-weighted, single-shot, and echo-planar pulse sequence, we collected functional images with the following parameters: repetition time = 2500 ms, echo time = 30 ms, flip angle = 80°, field of view = 240 × 240 mm, acquisition matrix = 80 × 80, voxel size = 3 mm isotropic, number of transverse inter-leaved slices = 46, and zero gap. Parameters for $T_1$-weighted imaging were: repetition time = 8.2 ms, echo time = 3.7 ms, flip angle = 8°, field of view = 240 × 240 mm, acquisition matrix = 240 × 240, voxel size = 1 mm isotropic, number of transverse inter-leaved slices = 170, and zero gap.

### dMRI acquisition

Using a single-shot spin echo planar imaging (EPI) sequence, whole brain dMRI images were acquired. Parameters of the sequence include: repetition time = 7748 ms, echo time = 86 ms, flip angle = 90°, diffusion gradient (monopolar) directions = 64, diffusion gradient timing DELTA/delta = 42.4/10 ms, *b* values: 0, 1000 s/mm$^2$, fat suppression using SPIR, field of view = 224 × 224 mm, in-plane resolution = 2 mm isotropic, number of transverse interleaved slices = 60, zero gap, slice thickness = 2 mm, SENSE factor = 2, and total acquisition time = 10 min 51 s.

### Force data analyses

Force data collected during task-based fMRI were filtered using a 10th-order Butterworth filter with a cutoff frequency of 15 Hz. For each force trial, we visually marked four time points: (1) onset of force, (2) time point to reach a steady-state hold, (3) time point to decrease force, and (4) offset of force. A custom MATLAB program (version R2013a; The Mathworks, Natick, MA) was used for computing three dependent variables: (a) mean force between time point (2) and (3), (b) rate of increase force: mean rate of change of force between (1) and (2), and (c) rate of decrease force: mean rate of change of force between (3) and (4).

### Task-based fMRI analyses

Using the Analysis of Functional NeuroImages software package (AFNI version 16.0.19; https://afni.nimh.nih.gov/afni/download/afni/psc_project_view) for functional data and Statistical Parametric Mapping (SPM8; http://www.fil.ion.ucl.ac.uk/spm/), we analyzed magnetic resonance imaging data. Before data analysis, we flipped structural and functional MRI data along the midline for participants who performed pinch grip force task with the left hand. Processing steps were consistent with our previous work (Burciu et al. 2015; Neely et al. 2015). A standard wholebrain (WB) analysis and a cerebellum-optimized analysis (a spatially unbiased atlas template of the cerebellum and brainstem: SUIT version

Author Manuscript Author Manuscript Author Manuscript Author Manuscript

3.1; http://www.diedrichsenlab.org/imaging/suit_download.htm) were executed (Diedrichsen 2006; Diedrichsen et al. 2009). The MNI_av152T1.nii template was used for whole-brain normalization, and the suit.nii template was used for the cerebellum normalization. We anatomically labeled significant fMRI clusters based on the human motor area template (HMAT) (Mayka et al. 2006), automated anatomical labeling (AAL) (Tzourio-Mazoyer et al. 2002), and probabilistic MRI atlas of the human cerebellum (Diedrichsen et al. 2009).

## Task-based functional connectivity analyses

Task-based functional connectivity analyses were performed on fMRI data including rest and task blocks using AFNI. Based on previous studies (Neely et al. 2015; Schurz et al. 2015), task-based functional connectivity was performed using a seed-based approach. Five cerebral cortex regions that showed significantly reduced BOLD activity, and significant correlation for BOLD activity and clinical assessments in SCA6 of this study were selected as seeds. These include: contralateral and ipsilateral SMA, contralateral and ipsilateral primary motor cortex (M1), and contralateral primary somatosensory cortex (S1). The steps were as follows: (a) despike to remove extreme time series outliers, (b) slice time correction for interleaved acquisition, (c) align EPI to the anatomy, (d) warp to MNI space, (e) segment anatomy into cerebral spinal fluid (CSF), gray matter and white matter, (f) regress data for CSF and whole brain signal, (g) process time series through ANATICOR (a pipeline of AFNI to project nuisance signals and localized transient hardware artifacts from EPI time series) (Jo et al. 2010), (h) censor time points with head motion >1.0 mm, and (i) smooth data with a 4 mm FWHM filter using the 3dBlurToFWHM function in AFNI. After obtaining the residual time series, we extracted the time series from the seed region and calculated correlation coefficients between the five seeds and other regions that were transformed to a z-score.

## dMRI analyses

Consistent with previous work (Ofori et al. 2015a, b, c), we performed preprocessing and analysis of dMRI data. The sequence of analysis follows: (a) using the FMRIB software Library (FSL version 5.0; Oxford, UK; http://fsl.fmrib.ox.ac.uk/fsldownloads/) and custom UNIX shell scripts we corrected signal distortions caused by eddy currents and head motion, compensated the diffusion gradients for these rotations, and removed non-brain tissues, (b) using custom code written in MATLAB we quantified free-water and corrected fractional anisotropy of the tissue compartment ($FA_T$) map from the preprocessed data, (c) data were normalized to MNI (Montreal Neurological Institute) space by using the b-zero image of each participant and warping this dataset to the MNI305 template (2 × 2 × 2 mm) (Fonov et al. 2011). This procedure used an affine transformation with 12 degrees of freedom and trilinear interpolation using FLIRT (http://fsl.fmrib.ox.ac.uk/fsl/fslwiki/FLIRT). Next, the resultant transformation matrix was used for normalizing the free-water and $FA_T$ maps to MNI space.

## Regions of interest

An experienced rater who was blind to group membership manually drew regions of interest (ROIs) on the b-zero image of each participant in MNI space. This approach has been validated as reliable in prior work (Planetta et al. 2015b; Prodoehl et al. 2013). Based on

Author Manuscript Author Manuscript Author Manuscript Author Manuscript

previous findings (Falcon et al. 2015; Vaillancourt et al. 2006), we selected seven ROIs important for visually-guided motor control and the size for each ROI was determined to cover the anatomy for all participants: (a) dentate nucleus (bilateral; 20 voxels), (b) superior cerebellar peduncle (bilateral; 14 voxels), (c) middle cerebellar peduncle (bilateral; 16 voxels), (d) inferior cerebellar peduncle (bilateral; 10 voxels), (e) lobule V (bilateral; 68 voxels), (f) lobule VI (bilateral; 125 voxels), and (g) vermis (42 voxels). Using the ROIs, we extracted the $FA_T$ and free-water values. Mean free-water and $FA_T$ values were calculated for bilateral ROIs in the dentate nucleus, superior, middle, and inferior cerebellar peduncles, and lobules V and VI (Fig. 4a). The vermis was a single ROI and spanned areas VIII and IX of the cerebellar lobules.

## Correlation analyses

Pearson's correlation was performed to determine relation between functional and structural changes in brain and clinical assessments of ataxia (ICARS kinetic, ICARS total, and SARA total). First, for fMRI data we calculated percent signal change (PSC) in nine regions of cerebral cortex and cerebellum that showed significantly different functional activity between SCA6 and controls in WB and SUIT analyses of this study. Mean values of PSC were computed from eight TRs (i.e., 17.5 s) consistent with the intermediate section of the force task (an average of the eight force blocks). Further, we included free-water values for the seven ROIs in the analysis. Thus, we computed relation between 16 brain imaging data (i.e., nine PSC values and seven free-water) and each clinical assessment. We used a false discovery rate (FDR) of $P < 0.05$ to make corrections for multiple comparisons (Benjamini–Hochberg–Yekutieli method available at http://www.mathworks.com/matlabcentral/fileexchange/27418-benjamini-hochbergyekutieliprocedurefor-controlling-false-discoveryrate/content/fdr_bh.m) (Benjamini and Hochberg 1995; Benjamini and Yekutieli 2001).

## Statistical analyses

Demographic and clinical data difference between groups were estimated pairwise using Pearson's Chi-squared test on sex, handedness, and hand tested, respectively, and Mann–Whitney *U* test on age, MVC, and MoCA. For each force variable, two-way mixed model 2 × 2 (Group: SCA6 and controls × Feedback: visual and no-visual feedback) ANOVAs with repeated measures on the last factor were applied. Moreover, mean free-water and $FA_T$ values within each ROI was averaged across side and then compared using independent *t* test to determine the difference between two groups ($P < 0.05$). All statistical analysis on demographic, clinical, force, and dMRI data was performed using IBM SPSS Statistics 22 (SPSS Inc., Chicago, IL, USA). Alpha level was corrected for multiple comparisons using the FDR procedure.

Statistical analyses on preprocessed fMRI data (functional activity) were performed within the framework of the general linear model using the six head motion parameters calculated during preprocessing as regressors of no interest; 2 × 2 mixed-effects ANOVA with two groups (controls vs. SCA6) and two visual feedback conditions (visual feedback vs. no-visual feedback). For task-based functional connectivity data, we used the 3dttest function in AFNI for comparing SCA6 vs. control. Using a Monte Carlo simulation with the AFNI's

Author Manuscript Author Manuscript Author Manuscript Author Manuscript

3dClustSim program, we corrected both functional activity and task-based functional connectivity data for preventing type I error and set the significant level of the contrasts of interest at the voxel level to $P < 0.005$ and a cluster (324 $mm^3$, providing corrected $P < 0.05$).

## Results

### Clinical and behavioral data

Pearson's Chi-square test on gender, handedness, and hand tested and Mann–Whitney $U$ test on age and pinch grip MVC showed no difference between SCA6 and age-matched healthy control groups (corrected $P$ value using a false discovery rate: $P_{FDR} > 0.05$; Table 1). SCA6 patients revealed significantly reduced MoCA scores than the control group (Mann–Whitney $U$ test: $P_{FDR} < 0.05$).

For force variables, two-way mixed model 2 × 2 (Group 9 Feedback) ANOVAs with repeated measures on the last factor revealed significant feedback main effects on mean force ($F_{1, 26} = 15.16$, $P = 0.001$), rate of force increase ($F_{1, 26} = 18.81$, $P < 0.001$), and rate of force decrease ($F_{1, 26} = 7.74$, $P = 0.01$). Specifically, the mean force, rate of force increase, and rate of force decrease were greater during no-visual feedback condition. No group main effect and interaction were found for the three dependent variables. The lack of behavioral differences on the task, suggest that the observations in fMRI are not being driven by group differences in task performance.

### Functional activity difference between groups: task-based fMRI data

ANOVA models on BOLD fMRI activity showed that pinch grip force control in the vision condition significantly increased BOLD activity in the bilateral primary and associative visual cortices, premotor and posterior parietal cortices, and midline structures of the cerebellum compared to pinch grip force control in the no vision condition. However, given that no Group × Feedback interactions were found, we report average of the BOLD signal changes collapsed across feedback conditions.

SCA6 patients revealed a tendency that BOLD signal in the sensorimotor cortex, SMA, and cerebellum was reduced in comparison to age-matched healthy individuals (Table 2; Supplementary Data Fig. 1). Specifically, bilateral regions of M1, SMA, and S1 showed less task-based functional activity for the SCA6 group. Moreover, a cerebellum-optimized analysis using the SUIT template revealed that BOLD signal in vermis VI, lobules I–IV, V, and VI were significantly reduced in SCA6 patients compared with controls (Fig. 2).

### Task-based functional connectivity

Figure 3 and Table 3 show task-based functional connectivity differences between SCA6 and control groups for the five sensorimotor cortex and SMA regions significantly correlated with severity of ataxic symptoms (see our correlation findings). The contralateral S1 revealed no significant difference in task-based functional connectivity between groups. However, task-based functional connectivity between contralateral M1 and SMA was decreased in SCA6 patients compared with controls. Further, less taskbased functional

Author Manuscript Author Manuscript Author Manuscript Author Manuscript

connectivity in SCA6 appeared between bilateral M1 and cerebellar regions (i.e., Vermis VI, lobule I–IV, V, and VI). Reduced task-based functional connectivity between bilateral SMA and cerebellar regions (i.e., Vermis VI, lobule I–IV, V, and VI) occurred in SCA6 patients (Fig. 3).

### Structural difference between groups: dMRI data

To determine structural changes in the cerebellum between SCA6 and control groups, we investigated the free-water values and $FA_T$ using dMRI data for dentate nucleus, superior, middle, and inferior cerebellar peduncles, lobules V and VI, and vermis. The independent t test showed that free-water values in SCA6 were significantly increased compared with controls for all seven ROIs of the cerebellum ($P_{FDR} < 0.05$; Fig. 4b). However, no significant difference in $FA_T$ appeared across the seven ROIs ($P_{FDR} > 0.05$; Fig. 4b).

### Relation between functional and structural changes and disease severity

In the SCA6 group, we examined the relation between functional changes of sensorimotor cortex, SMA, and cerebellar regions and structural (free-water values in seven ROIs of the cerebellum) and clinical measures of ataxia (i.e., ICARS and SARA). Figure 5 and Table 4 display significant correlation between severity of symptoms and functional activity in cerebral cortex regions (i.e., bilateral SMA, bilateral M1, and contralateral S1), and free-water values in superior cerebellar peduncle and lobule V. Reduced functional activity in the sensorimotor cortex and SMA was significantly related to more severe ataxic symptoms as indicated by higher ICARS kinetic, ICARS total, and SARA scores ($P_{FDR} < 0.05$). Further, elevated free-water values in superior cerebellar peduncle and lobule V were significantly correlated with increased scores in ICARS kinetic, ICARS total, and SARA ($P_{FDR} < 0.05$).

## Discussion

The poor recovery in SCA6 patients combined with the progressive nature of the disease may be a consequence of damage not only to the cerebellum but also to functionally interconnected brain structures critical to motor control. Using a robust pinch grip force control fMRI paradigm and free-water analyses of dMRI data, we found that SCA6 patients have: (a) widespread reduction in task-related functional activity across sensory and motor cortex including M1, S1, and SMA, and vermis and lobules I–VI of cerebellum, (b) reduced task-based functional connectivity between the cortical motor regions (M1 and SMA) and cerebellum (vermis and lobules I–VI), (c) elevated free-water in the cerebellum and importantly in the superior cerebellar peduncle, which is the efferent pathway, and (d) a strong relation of more severe ataxia symptoms in SCA6 to reduced functional activity in sensorimotor cortex and SMA and increased free-water in the superior cerebellar peduncle and lobule V. These findings point to widespread changes across sensorimotor cortex and cerebellum in SCA6.

Task-based fMRI analysis revealed that functional activity in SCA6 patients was extensively decreased throughout the sensorimotor cortex, SMA, and cerebellar regions. Specifically, bilateral M1, SMA, S1, vermis, and lobule I–VI were hypoactive in SCA6 patients compared with controls. Our results in the cerebellum are consistent with Stefanescu and

Author Manuscript Author Manuscript Author Manuscript Author Manuscript

colleagues' findings that functional activity in the cerebellar lobule V–VI decreased in individuals with cerebellar degeneration (SCA3, SCA6, and Friedreich's ataxia) compared with controls (Stefanescu et al. 2015). At the same time, we extend the literature by also showing reduced motor cortical activity in SCA6 compared with controls, and a strong relation between the functional activity in cortical regions (M1, SMA, and S1) and disease severity. Consistent with a previous fMRI-study in the patients with cerebellar ataxia (Stefanescu et al. 2015), no significant relation was found between functional activity in cerebellar regions and clinical ratings of ataxia. To our best knowledge, the current study is the first one to report functional changes in the sensorimotor cortex and SMA in relation to the severity of ataxic symptoms consistent with the hypothesis of extracerebellar damage advanced by Gierga and colleagues (Gierga et al. 2009).

Moreover, we explored task-based functional connectivity within motor cortex and between motor cortex and cerebellum regions. Across seed placed in bilateral M1, SMA, and contralateral S1, SCA6 patients showed decreased task-based functional connectivity between cortico-cortical regions (M1 vs. SMA) and cortical-cerebellar regions (M1 vs. Vermis VI and SMA vs. lobule V–VI). Falcon and colleagues reported that effective connectivity between visual-related cortex and intermediate and lateral cerebellum was reduced in individuals with more severe ataxic symptoms compared with healthy controls, presymptomatic, and mild SCA6 patients (Falcon et al. 2015). Our current findings provide new evidence that functional connectivity is also impaired in SCA6 in motor-related regions of the cortex and cerebellum.

For the first time in a cohort of SCA6 patients, free-water and $FA_T$ measures have been calculated based on dMRI data using a bi-tensor model. We found that free-water values in the seven ROIs (dentate nucleus, superior cerebellar peduncle, middle cerebellar peduncle, inferior cerebellar peduncle, lobule V and VI, and vermis) were significantly increased in SCA6 patients compared with age-matched healthy controls whereas the $FA_T$ values did not differ between two groups. These findings are consistent with the literature on Parkinson's disease (PD) which indicates: (a) higher free-water values in the posterior substantia nigra of PD than controls, but no difference in $FA_T$ values for PD (Ofori et al. 2015b) and (b) further elevation of free-water in the posterior substantia nigra of PD patients after 1 year (Ofori et al. 2015c). Given that free-water values could be associated with changes in diffusion across the extra-cellular space, and may relate to mechanisms such as atrophy, neuroinflammation, or altered cellular density (Maier-Hein et al. 2015; Pasternak et al. 2012; Wang et al. 2011), it is possible that free-water values are more sensitive than $FA_T$ for detecting changes in SCA6. It is also important to note that in a recent study examining patients with multiple system atrophy and progressive supranuclear palsy, free-water values in both of these diseases were elevated in the middle and superior cerebellar peduncles (Planetta et al. 2015b). Further, patients with PD did not have changes for free-water or $FA_T$ in the cerebellar peduncles. In the current study, we did not observe changes in $FA_T$ for SCA6; however, in the study of progressive supranuclear palsy it was found that $FA_T$ was substantially decreased in the superior cerebellar peduncle compared with PD and control subjects. The free-water value in the superior cerebellar peduncle of the progressive supranuclear palsy patients was on average equal to 0.66 (SD = 0.10), whereas the current study found free-water values equal to 0.46 (SD = 0.12) for SCA6 patients. It could be that

Author Manuscript Author Manuscript Author Manuscript Author Manuscript

free-water must elevate to a threshold before one observes reduced $FA_T$ values in regions such as the superior cerebellar peduncle, and that in the SCA6 subjects they could eventually exhibit reduced $FA_T$ as the disease progresses and becomes more severe.

By conducting correlation analyses on dMRI data in relation to clinical assessments, we observed a strong relation between free-water elevation in SCA6 and severity of disease symptoms. Specifically, elevated free-water values in the superior cerebellar peduncle and lobule V were significantly related to more severe ataxia symptoms as indicated by higher scores in ICARS and SARA. A significant relation between altered structural integrity in the cerebellum and disease severity is consistent with previous findings that reduced volume in the whole cerebellum, dentate, and superior cerebellar peduncle using structural MRI was correlated with increased ICARS and SARA scores for the patients with cerebellar ataxia (SCA3, SCA6, and Friedreich's ataxia) (Eichler et al. 2011; Sato et al. 2015; Stefanescu et al. 2015). Further, free-water values in the cerebellum may be an effective marker for estimating structural changes in relation to disease severity of SCA6 patients. The superior cerebellar peduncle is an efferent pathway and projects signals to the thalamus that relays signals to the primary motor cortex and premotor cortices (Watson et al. 2014). Moreover, lobule V receives input from M1 via the pons (Kelly and Strick 2003), and is relevant to upper extremity functions (Purves et al. 2012). Thus, the current findings indicate structural alterations not only in the cerebellar lobule but also impairment of the efferent pathways from the cerebellum to the motor cortex.

There were some limitations that are important to consider in this study. The current study focused on a handgrip motor control task, and the results may not extend to other effectors such as the oculomotor or lower limb. Further, we included right and left handed people given the rare nature of SCA6, and it is possible that including these samples influenced the current outcome. Finally, the relation between ataxia severity and both fMRI and dMRI outcomes were cross-sectional, and future longitudinal studies would be needed to confirm that these measures change over time.

In conclusion, the current study revealed decreased functional activity in M1, S1, SMA, cerebellar lobule I–VI, and cerebellar vermis along with elevated free-water values in superior cerebellar peduncle and lobule V of the cerebellum. Further, reduced functional activity in M1, S1, and SMA in addition to elevated free-water in superior cerebellar peduncle and lobule V, were strongly related to more severe ataxic symptoms. Collectively, these findings suggest that brain changes in SCA6 extend beyond the cerebellum, and point to functional and structural alterations along the cerebello-cortical pathways that are strongly related with the degree of motor severity observed in these patients.

## Supplementary Material

Refer to Web version on PubMed Central for supplementary material.

Author Manuscript Author Manuscript Author Manuscript Author Manuscript

## Acknowledgments

The authors would like to thank the participants and their families for their time and commitment to this research. This work was Supported by the National Institutes of Health (R01 NS075012, R01 NS058487, R21 NS093695, and T32 NS082168).

## References

Bastian AJ (2006) Learning to predict the future: the cerebellum adapts feedforward movement control. Curr Opin Neurobiol 16:645–649. doi:10.1016/j.conb.2006.08.016 [PubMed: 17071073]

Benjamini Y, Hochberg Y (1995) Controlling the false discovery rate: a practical and powerful approach to multiple testing. J Roy Stat Soc B Met 57:289–300

Benjamini Y, Yekutieli D (2001) The control of the false discovery rate in multiple testing under dependency. Ann Stat 29:1165–1188. doi:10.1214/aos/1013699998

Bernard JA et al. (2012) Resting state cortico-cerebellar functional connectivity networks: a comparison of anatomical and self-organizing map approaches. Front Neuroanat 6:31. doi:10.3389/Fnana.2012.00031 [PubMed: 22907994]

Bernard JA et al. (2014) Dissociable functional networks of the human dentate nucleus. Cereb Cortex 24:2151–2159. doi:10.1093/cercor/bht065 [PubMed: 23513045]

Burciu RG et al. (2015) Distinct patterns of brain activity in progressive supranuclear palsy and Parkinson's disease. Mov Disord 30:1248–1258. doi:10.1002/mds.26294 [PubMed: 26148135]

Diedrichsen J (2006) A spatially unbiased atlas template of the human cerebellum. Neuroimage 33:127–138. doi:10.1016/j.neuroimage.2006.05.056 [PubMed: 16904911]

Diedrichsen J, Balsters JH, Flavell J, Cussans E, Ramnani N (2009) A probabilistic MR Atlas of the human cerebellum. Neuroimage 46:39–46. doi:10.1016/j.neuroimage.2009.01.045 [PubMed: 19457380]

Eichler L, Bellenberg B, Hahn HK, Koster O, Schols L, Lukas C (2011) Quantitative assessment of brain stem and cerebellar atrophy in spinocerebellar ataxia types 3 and 6: impact on clinical status. Am J Neuroradiol 32:890–897. doi:10.3174/ajnr.A2387 [PubMed: 21372168]

Falcon MI, Gomez CM, Chen EE, Shereen A, Solodkin A (2015) Early cerebellar network shifting in spinocerebellar ataxia type 6. Cereb Cortex. doi:10.1093/cercor/bhv154

Fonov V, Evans AC, Botteron K, Almli CR, McKinstry RC, Collins DL (2011) Unbiased average age-appropriate atlases for pediatric studies. Neuroimage 54:313–327. doi:10.1016/j.neuroimage.2010.07.033 [PubMed: 20656036]

Gierga K et al. (2009) Spinocerebellar ataxia type 6 (SCA6): neurodegeneration goes beyond the known brain predilection sites. Neuropathol Appl Neurobiol 35:515–527. doi:10.1111/j.1365-2990.2009.01015.x [PubMed: 19207264]

Ilg W, Golla H, Thier P, Giese MA (2007) Specific influences of cerebellar dysfunctions on gait. Brain 130:786–798. doi:10.1093/brain/awl376 [PubMed: 17287287]

Jo HJ, Saad ZS, Simmons WK, Milbury LA, Cox RW (2010) Mapping sources of correlation in resting state FMRI, with artifact detection and removal. Neuroimage 52:571–582. doi:10.1016/j.neuroimage.2010.04.246 [PubMed: 20420926]

Kelly RM, Strick PL (2003) Cerebellar loops with motor cortex and prefrontal cortex of a nonhuman primate. J Neurosci 23:8432–8444 [PubMed: 12968006]

Maier-Hein KH et al. (2015) Widespread white matter degeneration preceding the onset of dementia. Alzheimers Dement 11:485–493. doi:10.1016/j.jalz.2014.04.518 [PubMed: 25035154]

Mayka MA, Corcos DM, Leurgans SE, Vaillancourt DE (2006) Three-dimensional locations and boundaries of motor and premotor cortices as defined by functional brain imaging: a meta-analysis. Neuroimage 31:1453–1474. doi:10.1016/j.neuroimage.2006.02.004 [PubMed: 16571375]

Middleton FA, Strick PL (2000) Basal ganglia and cerebellar loops: motor and cognitive circuits. Brain Res Rev 31:236–250. doi:10.1016/S0165-0173(99)00040-5 [PubMed: 10719151]

Morton SM, Bastian AJ (2004) Cerebellar control of balance and locomotion. Neuroscientist 10:247–259. doi:10.1177/1073858404263517 [PubMed: 15155063]

Author Manuscript Author Manuscript Author Manuscript Author Manuscript

Neely KA et al. (2015) Functional brain activity relates to 0–3 and 3–8 Hz force oscillations in essential tremor. Cereb Cortex 25:4191–4202. doi:10.1093/cercor/bhu142 [PubMed: 24962992]

Ofori E, Du G, Babcock D, Huang X, Vaillancourt DE (2015a) Parkinson's disease biomarkers program brain imaging repository. Neuroimage 124:1120–1124. doi:10.1016/j.neuroimage.2015.05.005 [PubMed: 25976927]

Ofori E et al. (2015b) Increased free water in the substantia nigra of Parkinson's disease: a single-site and multi-site study. Neurobiol Aging 36:1097–1104. doi:10.1016/j.neurobiolaging.2014.10.029 [PubMed: 25467638]

Ofori E et al. (2015c) Longitudinal changes in free-water within the substantia nigra of Parkinson's disease. Brain 138:2322–2331. doi:10.1093/brain/awv136 [PubMed: 25981960]

Pasternak O et al. (2012) Excessive extracellular volume reveals a neurodegenerative pattern in schizophrenia onset. J Neurosci 32:17365–17372. doi:10.1523/Jneurosci.2904-12.2012 [PubMed: 23197727]

Planetta PJ et al. (2015a) Distinct functional and macrostructural brain changes in Parkinson's disease and multiple system atrophy. Hum Brain Mapp 36:1165–1179. doi:10.1002/hbm.22694 [PubMed: 25413603]

Planetta PJ et al. (2015b) Free-water imaging in Parkinson's disease and atypical parkinsonism. Brain. doi:10.1093/brain/awv361

Prodoehl J et al. (2013) Diffusion tensor imaging of Parkinson's disease, atypical parkinsonism, and essential tremor. Mov Disord 28:1816–1822. doi:10.1002/mds.25491 [PubMed: 23674400]

Purves D, Augustine GJ, Fitzpatrick D, Hall WC, LaMantia AS, White LE (2012) Neuroscience, 5th edn. Sinauer Association Inc, Sunderland

Reetz K et al. (2013) Genotype-specific patterns of atrophy progression are more sensitive than clinical decline in SCA1, SCA3, and SCA6. Brain 136:905–917. doi:10.1093/brain/aws369 [PubMed: 23423669]

Sato K, Ishigame K, Ying SH, Oishi K, Miller MI, Mori S (2015) Macro- and microstructural changes in patients with spinocerebellar ataxia type 6: assessment of phylogenetic subdivisions of the cerebellum and the brain stem. AJNR Am J Neuroradiol 36:84–90. doi:10.3174/ajnr.A4085 [PubMed: 25169926]

Schurz M, Wimmer H, Richlan F, Ludersdorfer P, Klackl J, Kronbichler M (2015) Resting-state and task-based functional brain connectivity in developmental dyslexia. Cereb Cortex 25:3502–3514. doi:10.1093/cercor/bhu184 [PubMed: 25169986]

Seidel K, Siswanto S, Brunt ERP, den Dunnen W, Korf HW, Rub U (2012) Brain pathology of spinocerebellar ataxias. Acta Neuropathol 124:1–21. doi:10.1007/s00401-012-1000-x [PubMed: 22684686]

Shadmehr R, Krakauer JW (2008) A computational neuroanatomy for motor control. Exp Brain Res 185:359–381. doi:10.1007/s00221008-1280-5 [PubMed: 18251019]

Solodkin A, Gomez CM (2012) Spinocerebellar ataxia type 6. Handb Clin Neurol 103:461–473. doi:10.1016/B978-0-444-51892-7.00029-2 [PubMed: 21827907]

Spraker MB, Prodoehl J, Corcos DM, Comella CL, Vaillancourt DE (2010) Basal ganglia hypoactivity during grip force in drug naive Parkinson's disease. Hum Brain Mapp 31:1928–1941. doi:10.1002/hbm.20987 [PubMed: 20225221]

Stefanescu MR et al. (2015) Structural and functional MRI abnormalities of cerebellar cortex and nuclei in SCA3, SCA6 and Friedreich's ataxia. Brain 138:1182–1197. doi:10.1093/brain/awv064 [PubMed: 25818870]

Tuite PJ, Dagher A (2013) Magnetic resonance imaging in movement disorders: a guide for clinicians and scientists. Cambridge University, Cambridge

Tzourio-Mazoyer N et al. (2002) Automated anatomical labeling of activations in SPM using a macroscopic anatomical parcellation of the MNI MRI single-subject brain. Neuroimage 15:273–289. doi:10.1006/nimg.2001.0978 [PubMed: 11771995]

Vaillancourt DE, Mayka MA, Corcos DM (2006) Intermittent visuomotor processing in the human cerebellum, parietal cortex, and premotor cortex. J Neurophysiol 95:922–931. doi:10.1152/jn.00718.2005 [PubMed: 16267114]

Author Manuscript Author Manuscript Author Manuscript Author Manuscript

Wang Y et al. (2011) Quantification of increased cellularity during inflammatory demyelination. Brain 134:3587–3598. doi:10.1093/brain/awr307

Watson TC, Becker N, Apps R, Jones MW (2014) Back to front: cerebellar connections and interactions with the prefrontal cortex. Front Syst Neurosci 8:4. doi:10.3389/fnsys.2014.00004 [PubMed: 24550789]

Author Manuscript Author Manuscript Author Manuscript Author Manuscript

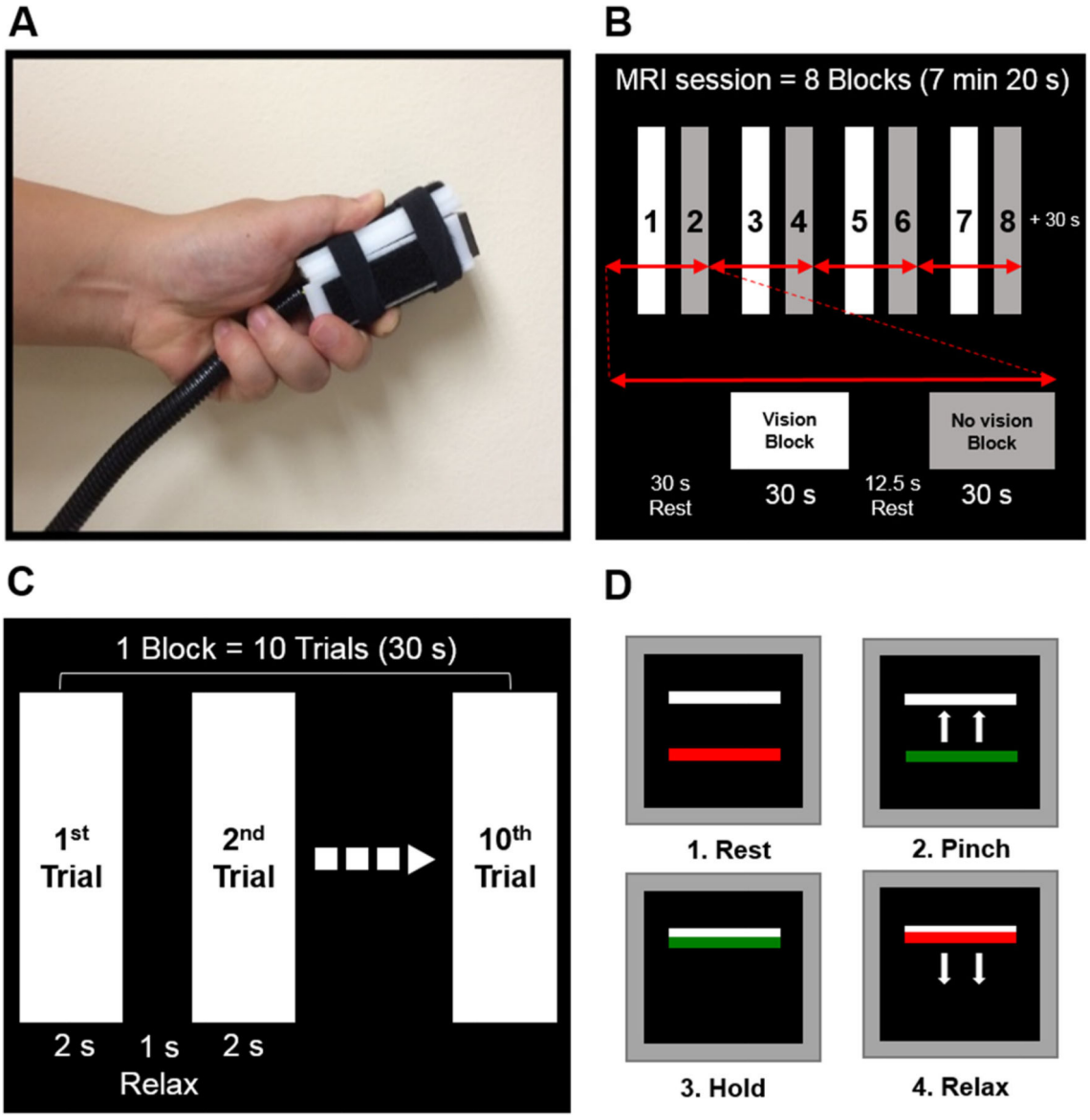


**Fig. 1.**

Pinch grip force control task in MRI scanner. Grip force apparatus (**a**). MRI session with eight *blocks* (**b**). *Block* design including 10 trials (**c**). Visually guided force control task (**d**)

Author Manuscript Author Manuscript Author Manuscript Author Manuscript

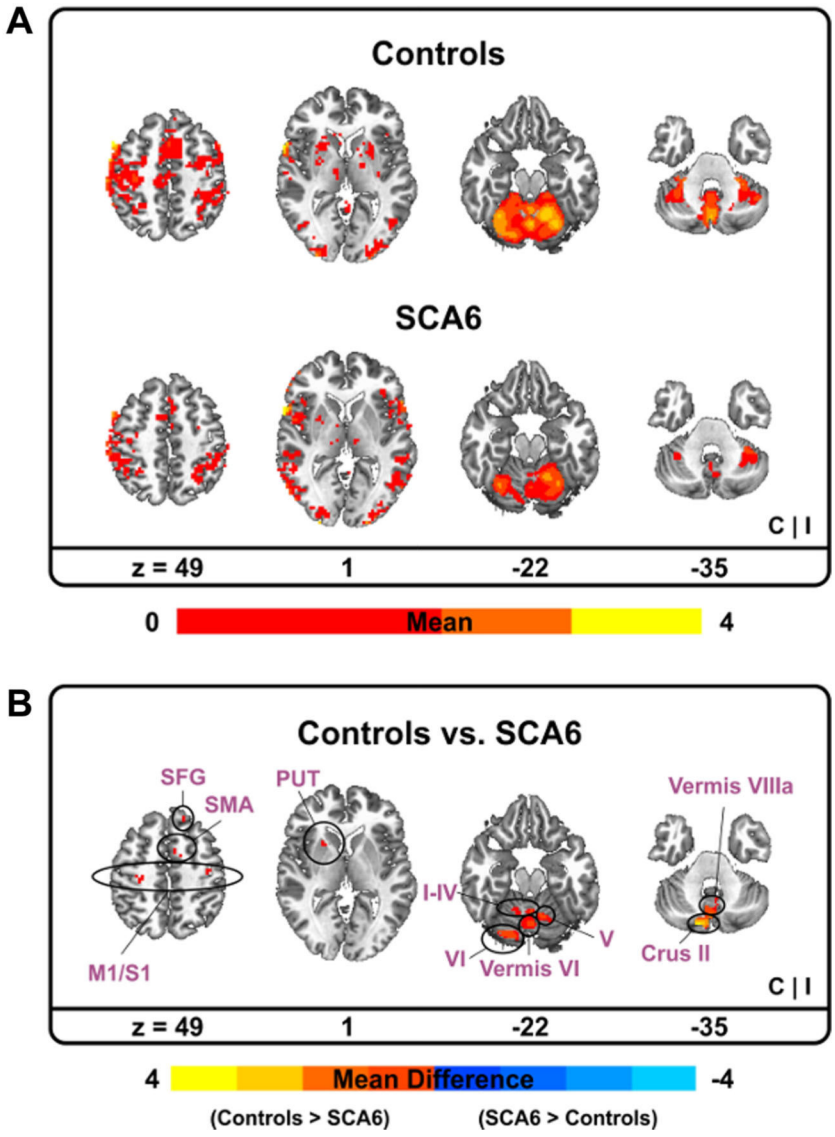


**Fig. 2.**

Functional MRI results between SCA6 and controls. Functional activity for each group. *Warm (yellow) colors* indicate where BOLD (blood oxygen level-dependent) activity was positive (**a**). Functional activity difference between two groups. *Warm (yellow) colors* indicate where BOLD activity in controls was greater than SCA6 whereas *cold (blue) colors* denote where BOLD activity in controls was less than SCA6 (**b**). *C* contralateral hemisphere, *I* ipsilateral hemisphere, *M1* primary motor cortex, *PUT* putamen, *S1* primary somatosensory cortex, *SFG* superior frontal gyrus, *SMA* supplementary motor area

Author Manuscript Author Manuscript Author Manuscript Author Manuscript

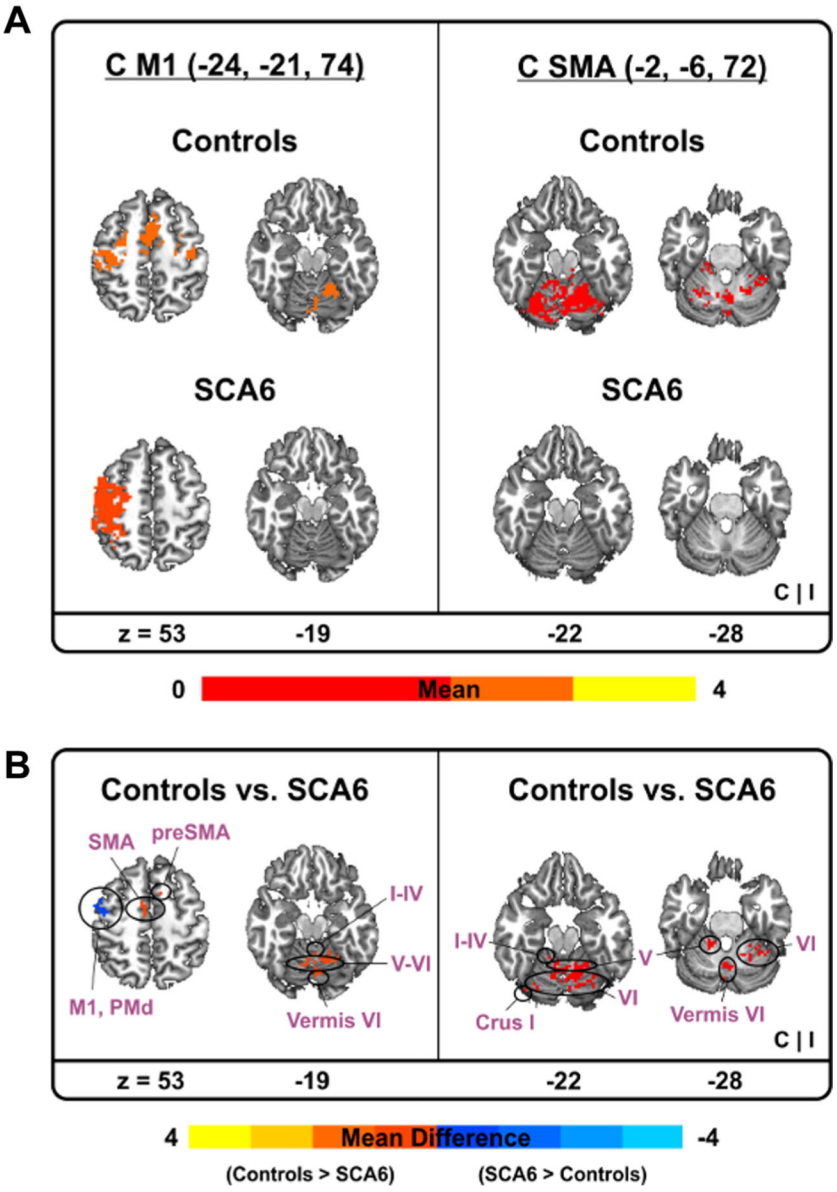


**Fig. 3.**

Task-based functional connectivity results between SCA6 and controls. Task-based functional connectivity between contralateral M1 vs. cerebellum (*left*) and contralateral SMA vs. cerebellum (*right*). *Warm (yellow) colors* indicate where task-based functional connectivity was positive (**a**). Task-based functional connectivity difference between two groups. *Warm (yellow) colors* indicate where task-based functional connectivity in controls was greater than SCA6 whereas *cold (blue) colors* denote where task-based functional connectivity in controls was less than SCA6 (**b**). *C* contralateral hemisphere, *I* ipsilateral hemisphere

Author Manuscript Author Manuscript Author Manuscript Author Manuscript

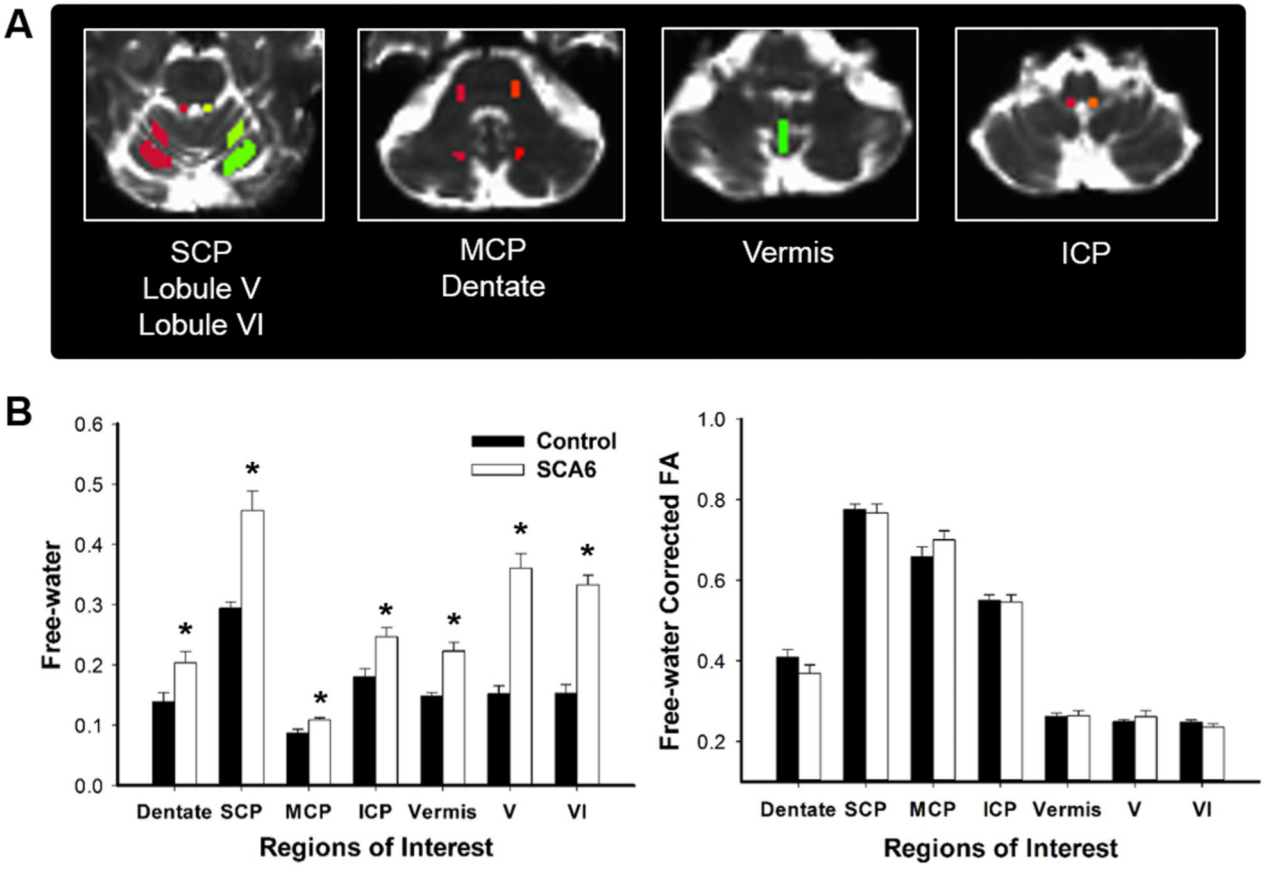


**Fig. 4.**

Regions of interest (ROIs) and diffusion MRI results. Seven ROIs in the cerebellum (**a**). Free-water values (*left*) and free-water corrected fractional anisotropy ($FA_T$; *right*) between SCA6 and controls (**b**). *ICP* inferior cerebellar peduncle, *195:256MCP* middle cerebellar peduncle, *SCP* superior cerebellar peduncle. Data represent mean ± standard error

Author Manuscript Author Manuscript Author Manuscript Author Manuscript

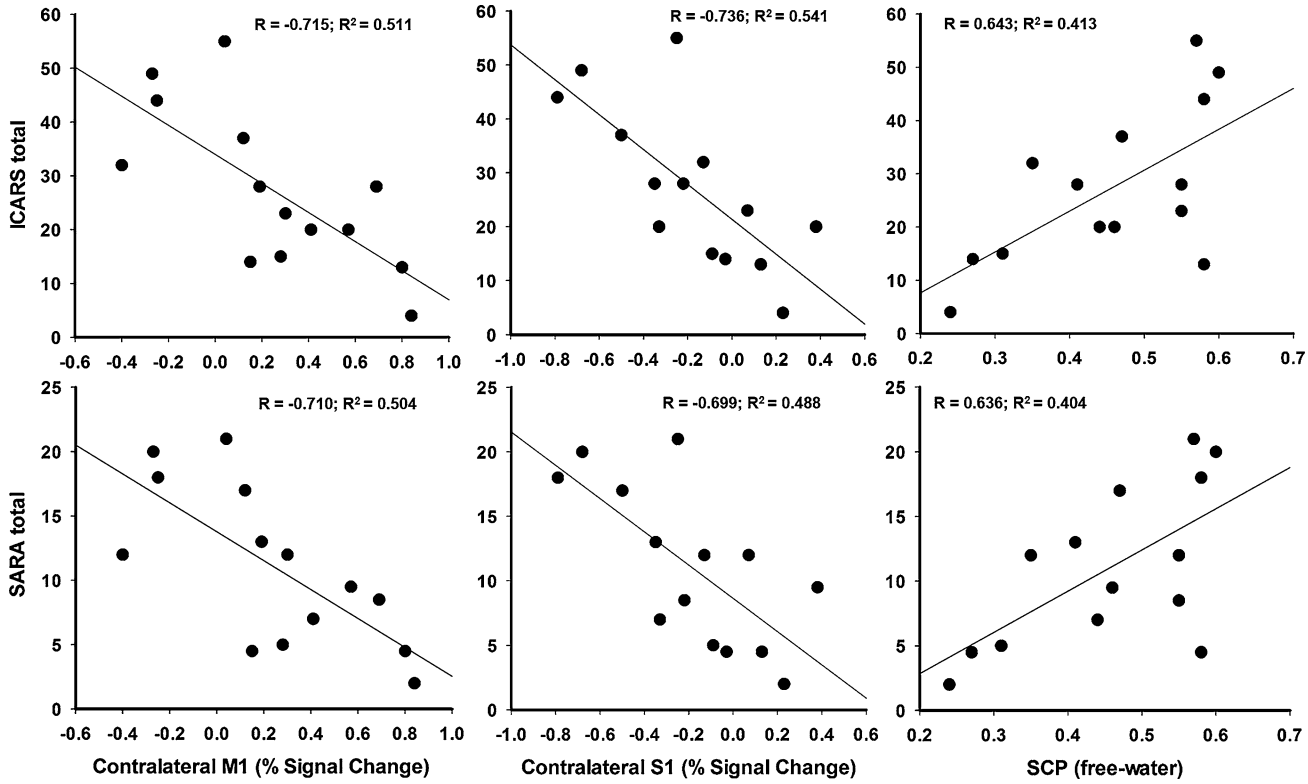


**Fig. 5.**

Representative relation between functional and structural changes in brain and ataxia severity. Percent signal change in the sensorimotor cortex (M1 and S1) notes changes in functional activity. Free-water values in the superior cerebellar peduncle (SCP) indicate structural changes. Clinical assessments for ataxia include ICARS (*scale* = 0–100) and SARA (*scale* = 0–40) total values; *higher scores* indicate more severe ataxia symptoms

Author Manuscript Author Manuscript Author Manuscript Author Manuscript



**Table 1**

Demographic and clinical characteristics

| **Demographics** | **Control (*N* = 14)** | **SCA6 (*N* = 14)** | **$P_{FDR}$ value** |
|---|---|---|---|
| Sex (female: male) | 10:4 | 10:4 | 1.00 |
| Handedness (left: right) | 1:13 | 4:10 | 0.56 |
| Hand tested (left: right) | 4:10 | 5:9 | 0.82 |
| Age (years) | 63.6 (6.8) | 65.8 (7.9) | 0.82 |
| MVC (*N*) | 64.1 (18.8) | 50.1 (24.1) | 0.23 |
| MoCA: total | 27.4 (1.5) | 24.5 (2.9) | 0.02 |
| ICARS: kinetic | - | 10.4 (6.2) | - |
| ICARS: total | - | 27.3 (14.8) | - |
| SARA: total | - | 11.0 (6.2) | - |

Data are sums or means (±SD)

Note that handedness was self-reported; more affected hand, which was self-reported, was used for SCA6 and either dominant or non-dominant hand assigned randomly was used for controls

*ICARS* International Cooperative Ataxia Rating Scale, *MoCA* montreal cognitive assessment, *MVC* maximum voluntary contraction, $P_{FDR}$ corrected *P* value using a false discovery rate, *SARA* scale for the assessment and rating of ataxia, *SCA6* spinocerebellar ataxia type 6

*Brain Struct Funct*. Author manuscript; available in PMC 2018 December 03.

Author Manuscript Author Manuscript Author Manuscript Author Manuscript



*Brain Struct Funct*. Author manuscript; available in PMC 2018 December 03.

**Table 2**

Cerebral and cerebellar fMRI activation differences between control and SCA6 groups

| Brain region (s) | Side | Size ($mm^3$) | MNI coordinates (Peak) | | | *F* value |
|---|---|---|---|---|---|---|
| | | | *x* | *y* | *z* | |
| Whole brain analysis | | | | | | |
| CON > SCA6 | | | | | | |
| Middle frontal gyrus; PMv | I | 1728 | 45 | 30 | 36 | 9.04 |
| Superior frontal gyrus | C | 1701 | −27 | 51 | 18 | 15.70 |
| | C | 324 | −18 | 66 | 21 | 24.02 |
| Putamen | C | 1161 | −24 | 9 | −6 | 16.11 |
| Caudate nucleus | C | 567 | −24 | −3 | 18 | 21.32 |
| SMA, preSMA | C | 378 | −2 | −6 | 72 | 12.38 |
| | I | 351 | 3 | −3 | 57 | 11.99 |
| Precentral gyrus; M1 | C | 918 | −24 | −21 | 74 | 13.93 |
| | C | 621 | −30 | −24 | 51 | 16.19 |
| | I | 324 | 27 | −15 | 72 | 20.02 |
| Postcentral gyrus; S1 | C | 432 | −33 | −36 | 69 | 9.88 |
| | I | 1161 | 39 | −31 | 63 | 8.99 |
| Superior parietal lobule | C | 378 | −36 | −48 | 69 | 12.05 |
| Middle cingulate cortex | C | 351 | −9 | −30 | 51 | 33.41 |
| SCA6 > CON | I | 324 | 12 | −90 | −12 | 10.69 |
| Temporal pole | I | 486 | 51 | 21 | −18 | 18.93 |
| Lingual gyrus | I | 324 | 12 | −90 | −12 | 10.69 |
| SUIT analysis: cerebellum | I | 324 | 12 | −90 | −12 | 10.69 |
| CON > SCA6 | I | 324 | 12 | −90 | −12 | 10.69 |
| Vermis VI, lobule I-IV, V, VI | | 6248 | 0 | −66 | −17 | 28.76 |
| Crus I-II, VIIb, vermis VIIIa/b | C | 6048 | −12 | −80 | −45 | 28.23 |

*C* contralateral hemisphere, *CON* control, *I* ipsilateral hemisphere, *M1* primary motor cortex, *MNI* Montreal Neurological Institute, *PMv* ventral premotor, *S1* primary somatosensory cortex, *SMA* supplementary motor area, *SCA6* spinocerebellar ataxia type 6

Author Manuscript Author Manuscript Author Manuscript Author Manuscript



**Table 3**

Difference of task-based functional connectivity between control and SCA6 groups

| Brain region (s) | Side | Size ($mm^3$) | MNI coordinates (Peak) | | | *t* value |
|---|---|---|---|---|---|---|
| | | | *x* | *y* | *z* | |
| M1 (−24, −21, 74) | C | | | | | |
| CON > SCA6 | | | | | | |
| Vs. vermis VI, Lobule I–IV, V, VI | | 3294 | 3 | −66 | −15 | 6.40 |
| Vs. SMA | C | 378 | −9 | −3 | 54 | 4.14 |
| Vvs. SMA, preSMA | I | 378 | 6 | 9 | 51 | 3.83 |
| SCA6 > CON | | | | | | |
| Vs. M1, PMd | C | 675 | −45 | −9 | 57 | 3.41 |
| M1 (27, −15, 72) | I | | | | | |
| CON > SCA6 | | | | | | |
| Vs. vermis VI | | 648 | 3 | −66 | −12 | 3.30 |
| SMA, preSMA (−2, −6, 72) | C | | | | | |
| CON > SCA6 | | | | | | |
| Vs. vermis VI, Lobule I–IV, V, VI | I | 4995 | 24 | −66 | −18 | 4.21 |
| Vs. lobule VI | I | 486 | 36 | −48 | −30 | 3.94 |
| Vs. crus I | C | 324 | −42 | −72 | −24 | 4.73 |
| SMA (3, −3, 57) | I | | | | | |
| CON > SCA6 | | | | | | |
| Vs. lobule V | I | 2376 | 9 | −57 | −15 | 5.62 |

*C* contralateral hemisphere, *CON* control, *I* ipsilateral hemisphere, *M1* primary motor cortex, *MNI* Montreal Neurological Institute, *PMd* dorsal premotor, *SMA* supplementary motor area, *SCA6* spinocerebellar ataxia type 6

*Brain Struct Funct*. Author manuscript; available in PMC 2018 December 03.

Author Manuscript Author Manuscript Author Manuscript Author Manuscript



**Table 4**

Correlation between structural and functional changes in brain and ataxia severity

| Brain region (s) | ICARS kinetic | ICARS total | SARA total |
|---|---|---|---|
| BOLD: percent signal change (MNI Coordinates) | | | |
| cM1 (−24, −21, 74) | −0.698* ($P_{FDR}$ = 0.02) | −0.715* ($P_{FDR}$ = 0.03) | −0.710* ($P_{FDR}$ = 0.04) |
| cM1 (−30, −24, 51) | −0.443 ($P_{FDR}$ = 0.19) | −0.407 ($P_{FDR}$ = 0.24) | −0.476 ($P_{FDR}$ = 0.14) |
| iM1 (27, −15, 72) | −0.676* ($P_{FDR}$ = 0.03) | −0.618* ($P_{FDR}$ = 0.04) | −0.632* ($P_{FDR}$ = 0.04) |
| cSMA, preSMA (−2, −6, 72) | −0.718* ($P_{FDR}$ = 0.02) | −0.618* ($P_{FDR}$ = 0.04) | −0.598 ($P_{FDR}$ = 0.05) |
| iSMA (3, −3, 57) | −0.723* ($P_{FDR}$ = 0.02) | −0.633* ($P_{FDR}$ = 0.04) | −0.667* ($P_{FDR}$ = 0.04) |
| cS1 (−33, −36, 69) | −0.802* ($P_{FDR}$ = 0.02) | −0.736* ($P_{FDR}$ = 0.03) | −0.699* ($P_{FDR}$ = 0.04) |
| iS1 (39, −31, 63) | −0.376 ($P_{FDR}$ = 0.27) | −0.302 ($P_{FDR}$ = 0.39) | −0.335 ($P_{FDR}$ = 0.32) |
| Vermis VI, Lobule V-VI (0, −66, −17) | −0.172 ($P_{FDR}$ = 0.60) | −0.084 ($P_{FDR}$ = 0.86) | −0.011 ($P_{FDR}$ = 1.00) |
| Crus I-II, VIIb, Vermis VIIIa/b (−12, −80, −45) | −0.197 ($P_{FDR}$ = 0.57) | −0.178 ($P_{FDR}$ = 0.67) | −0.157 ($P_{FDR}$ = 0.73) |
| Free-water | | | |
| Dentate nucleus | 0.439 ($P_{FDR}$ = 0.19) | 0.582 ($P_{FDR}$ = 0.05) | 0.583 ($P_{FDR}$ = 0.06) |
| SCP | 0.572 ($P_{FDR}$ = 0.07) | 0.643* ($P_{FDR}$ = 0.04) | 0.636* ($P_{FDR}$ = 0.04) |
| MCP | 0.518 ($P_{FDR}$ = 0.12) | 0.579 ($P_{FDR}$ = 0.05) | 0.496 ($P_{FDR}$ = 0.13) |
| ICP | −0.222 ($P_{FDR}$ = 0.55) | 0.001 ($P_{FDR}$ = 1.00) | 0.002 ($P_{FDR}$ = 1.00) |
| Vermis | −0.112 ($P_{FDR}$ = 0.70) | 0.074 ($P_{FDR}$ = 0.86) | 0.102 ($P_{FDR}$ = 0.83) |
| Lobule V | 0.586 ($P_{FDR}$ = 0.07) | 0.630* ($P_{FDR}$ = 0.04) | 0.631* ($P_{FDR}$ = 0.04) |
| Lobule VI | 0.329 ($P_{FDR}$ = 0.33) | 0.359 ($P_{FDR}$ = 0.30) | 0.349 ($P_{FDR}$ = 0.32) |

Data are correlation coefficient ($P_{FDR}$)

*BOLD* blood oxygen level-dependent, *c* contralateral, *i* ipsilateral, *ICARS* International Cooperative Ataxia Rating Scale, *ICP* inferior cerebellar peduncle, *M1* primary motor cortex, *MCP* middle cerebellar peduncle, *MNI* Montreal Neurological Institute, $P_{FDR}$ corrected *P* value using a false discovery rate, *S1* primary somatosensory cortex, *SARA* scale for the assessment and rating of ataxia, *SCP* superior cerebellar peduncle, *SMA* supplementary motor area

*Indicates significant correlation ($P_{FDR} < 0.05$)

*Brain Struct Funct*. Author manuscript; available in PMC 2018 December 03.